Environ Monit Assess (2026) 198:2
https://doi.org/10.1007/s10661-025-14858-x

RESEARCH

Long-term assessment of PM_{10} and SO_2 in northwestern Türkiye: meteorology, inversions, and transboundary transport

Atilla Mutlu

Received: 19 September 2025 / Accepted: 22 November 2025 / Published online: 2 December 2025

Abstract This study provides a comprehensive long-term assessment of air quality in Balıkesir, northwestern Türkiye, focusing on the spatiotemporal variability of PM_{10} and SO_2 during 2013–2023. The analysis integrates pollutant observations with ERA5 reanalysis meteorological data to examine seasonal and diurnal variations, long-term trends, and the role of temperature inversions and atmospheric circulation in shaping pollution episodes. Results indicate that both pollutants reach their highest concentrations in winter due to intensified domestic heating and stagnant meteorological conditions, with temperature inversions acting as a key driver of near-surface accumulation. The Theil–Sen trend analysis revealed an insignificant long-term change in PM_{10} but a statistically significant upward trend in SO_2 ($+0.5$ μg m^{-3} $year^{-1}$), suggesting persistent reliance on sulfur-rich fuels during the cold season. However, a short-term decline after 2020 reflected the combined effects of cleaner fuels and pandemic-related emission reductions. Correlation analysis demonstrated that PM_{10} and SO_2 are moderately interrelated ($r = 0.49$) and primarily controlled by high-pressure, low-wind conditions. HYSPLIT trajectory analyses confirmed that severe winter episodes result from the combined influence of local stagnation and regional air mass transport. These findings highlight the dual importance of emission control and meteorological monitoring in managing winter pollution. Policy recommendations include stricter regulation of heating fuels, inversion-based early-warning systems, and enhanced regional cooperation to mitigate transported particulate matter.

Keywords Air quality · Long-range transport · HYSPLIT · PM_{10} · SO_2 · Trends

Introduction

Air pollution is a critical environmental issue impacting human health, ecosystems, and the climate (Araujo et al., 2020; Kalantari et al., 2024; Khaslan et al., 2024). Among the numerous pollutants, airborne particulate matter (PM_{10}) and sulfur dioxide (SO_2) are particularly concerning because of their ability to penetrate deep into the respiratory system and cause long-term health effects (Mai, 2024; Opeoluwa Oluwanifemi et al., 2024). Understanding the behavior of these pollutants in relation to meteorological drivers is essential for developing effective air-quality management strategies (Huang et al., 2021). According to the World Health Organization, both short- and long-term exposures to PM_{10} and SO_2 remain a global public-health challenge (WHO, 2021).

A. Mutlu (✉)
Department of Environmental Engineering, Balikesir University, Çağış, Balıkesir 10145, Turkey
e-mail: amutlu@balikesir.edu.tr

To contextualize the observed concentrations, Table 1 summarizes the main international and national air-quality standards for PM_{10} and SO_2. The World Health Organization (WHO) recommends much lower guideline values than regional legal limits, reflecting stricter health-based evidence. The European Union Air Quality Directive 2008/50/EC and the Turkish National Air Quality Regulation (No. 2008/29212; updated 2023) adopt intermediate thresholds that remain legally enforceable within Türkiye. Comparing measured concentrations with these benchmarks highlights both the environmental and public-health significance of exceedances observed in this study.

Over the past two decades, international air-quality standards have undergone a gradual but important tightening in response to accumulating epidemiological evidence linking fine and coarse particulate matter, as well as sulfur dioxide, to adverse health outcomes. The WHO guidelines represent a significant downward revision compared with the 2005 version, lowering the annual PM_{10} limit from 20 to 15 μg m^{-3} and the 24-h SO_2 limit from 20 μg m^{-3} (as interim guidance) to 40 μg m^{-3}. In contrast, the EU Directive (2008/50/EC) and Turkish National Regulation (HKDY, 2008) maintain comparatively higher legal thresholds (40 μg m^{-3} annual PM_{10}; 125 μg m^{-3} daily SO_2), reflecting both regulatory feasibility and regional socio-economic contexts. These differences illustrate a persistent gap between health-based recommendations and enforceable air-quality objectives. By comparing observed concentrations in Balıkesir with these evolving benchmarks, the present study highlights where air quality still exceeds the most protective WHO levels, emphasizing the need for continued policy alignment and emission control strategies to meet future public-health targets.

Meteorology plays a crucial role in determining the spatiotemporal variability of air pollutants. Parameters such as temperature, wind speed, wind direction, and atmospheric pressure are not passive background conditions but active factors that regulate pollutant dispersion or accumulation (Guo et al., 2022; Yang & Shao, 2021). During winter months, meteorological phenomena such as temperature inversions, stagnant air masses, and high-pressure systems trap pollutants near the surface, exacerbating their harmful impacts (Behera & Gokhale, 2024; Kumar et al., 2022; Lagmiri & Dahech, 2024; Rodrigues et al., 2021; Zhang et al., 2021; Zhou et al., 2024).

Additional international studies further illustrate these dynamics: long-term analyses in East Asia and Europe show that boundary-layer stability and weak-wind episodes lead to sharp PM_{10} and SO_2 increases (Masoud, 2023; Park et al., 2019; van Pinxteren et al., 2019), while research in Southeast Asia links severe haze events to meteorological anomalies and transboundary transport (Iqbal et al., 2025).

Although considerable progress has been made in air-quality research globally, significant knowledge gaps persist (Aas et al., 2024; Imam et al., 2024; Sokhi et al., 2021; Tang et al., 2024). Several gaps therefore need to be addressed. First, the long-term seasonal and diurnal variations of PM_{10} and SO_2 in Balıkesir have not been systematically analyzed in connection with inversion conditions and

Table 1 Comparison of WHO, EU, and Turkish limit values for PM_{10} and SO_2 levels

Pollutant	Averaging period	WHO Guideline (2021)[a]	EU Directive 2008/50/EC[b]	Türkiye National Regulation (2008)[c]	Health Implication Reference
PM_{10}	24 h	45 μg m^{-3}	50 μg m^{-3} (≤ 35 days yr^{-1})	50 μg m^{-3} (≤ 35 days yr^{-1})	Short-term respiratory morbidity
	Annual	15 μg m^{-3}	40 μg m^{-3}	40 μg m^{-3}	Chronic cardiovascular & pulmonary impacts
SO_2	24 h	40 μg m^{-3}	125 μg m^{-3} (≤ 3 days yr^{-1})	125 μg m^{-3} (≤ 3 days yr^{-1})	Acute respiratory irritation
	Hourly (max)	—	350 μg m^{-3} (≤ 24 days yr^{-1})	350 μg m^{-3} (≤ 24 days yr^{-1})	Short-term exposure peaks

[a](WHO, 2021)

[b](EU, 2008)

[c](HKDY, 2008)

wind components. Second, while compliance with European Union (EU) standards for PM_{10} and SO_2 has been studied in other regions (Cichowicz & Dobrzański, 2021; Lembo et al., 2021; Robotto et al., 2022; Sicard et al., 2021), few studies have integrated robust statistical trend detection with meteorological diagnostics. Third, regional and transboundary influences remain under-quantified. Recent work in Türkiye and surrounding regions demonstrates the importance of considering both local and transported contributions: desert-dust incursions and synoptic flow have been shown to elevate PM_{10} and SO_2 levels (Bhardwaj et al., 2019; Bodor et al., 2020; Dogan & Atbinici, 2022; Javed et al., 2022).

This study aims to fill these gaps by conducting a comprehensive analysis of PM_{10} and SO_2 pollution in Balıkesir between 2013 and 2023. Specifically, it

- evaluates seasonal and diurnal variations of both pollutants,
- detects long-term trends using the Theil–Sen estimator,
- investigates the influence of temperature inversions and wind components on pollution episodes, and
- applies HYSPLIT trajectory modeling to identify the contributions of regional and long-range transport.

To our knowledge, this is the first long-term integrated study in northwestern Türkiye combining meteorological analysis, inversion dynamics, and trajectory modeling. The findings are expected to inform targeted local mitigation strategies and regional cooperation efforts for improved air quality.

Methodology

Study area

Balıkesir Province is located in northwestern Türkiye (39° N, 28° E), occupying a transition zone between the Marmara and Aegean regions with a total area of approximately 14,300 km^2. The province extends from the coastal lowlands of the Marmara Sea in the north (0–100 m a.s.l.) to interior basins and hilly terrain exceeding 1000 m a.s.l. toward the Kazdağları (Mt. Ida) range in the west and Dursunbey–Simav highlands in the southeast. This complex topography forms alternating plains and ridges that strongly modulate air-mass movement and pollutant dispersion. The main urban center of Balıkesir lies in a shallow basin (~ 140 m a.s.l.) surrounded by gentle hills, which promotes nocturnal temperature inversions and pollutant trapping under calm-wind, high-pressure conditions—particularly during winter (BCAAP, 2024).

The coastal districts (Bandırma, Erdek) experience maritime air influence and frequent sea-breeze circulations, enhancing pollutant ventilation, whereas inland valleys often exhibit reduced mixing heights and stagnation episodes. Regional wind climatology is dominated by northeasterly (Poyraz) and southwesterly (Lodos) flows that control both local recirculation and potential long-range transport from the Marmara industrial corridor. Including these orographic and meteorological descriptors provides a physical basis for interpreting the spatial variability and episodic accumulation of PM_{10} and SO_2 concentrations observed in this study.

Figure 1 illustrates the location of the study area in northwestern Türkiye and provides a detailed aerial view of Balıkesir city, showing the Air Quality Monitoring Station (AQMS), downtown area, airport, and industrial park. The map includes coordinate gridlines, a north arrow, and a scale bar for spatial reference. The background satellite imagery (© Google Earth, 2025) offers a clear topographical overview, highlighting the basin-like setting that influences local air-pollution dispersion and accumulation.

As illustrated in Fig. 1, the Air Quality Monitoring Station (AQMS) is marked in red and is located near the downtown area of Balıkesir. The regional meteorological observation site, shown in blue, is situated within the local airport area in the southeastern part of the city, where on-site meteorological data are regularly recorded. Additionally, an industrial park of medium scale is located southwest of the city, highlighted in orange, representing the main industrial emission zone that may influence local air quality. These locations collectively define the principal monitoring and emission areas considered in this study.

Data overview

The dataset comprises hourly measurements spanning 2013–2023; unless otherwise noted, analyses focus

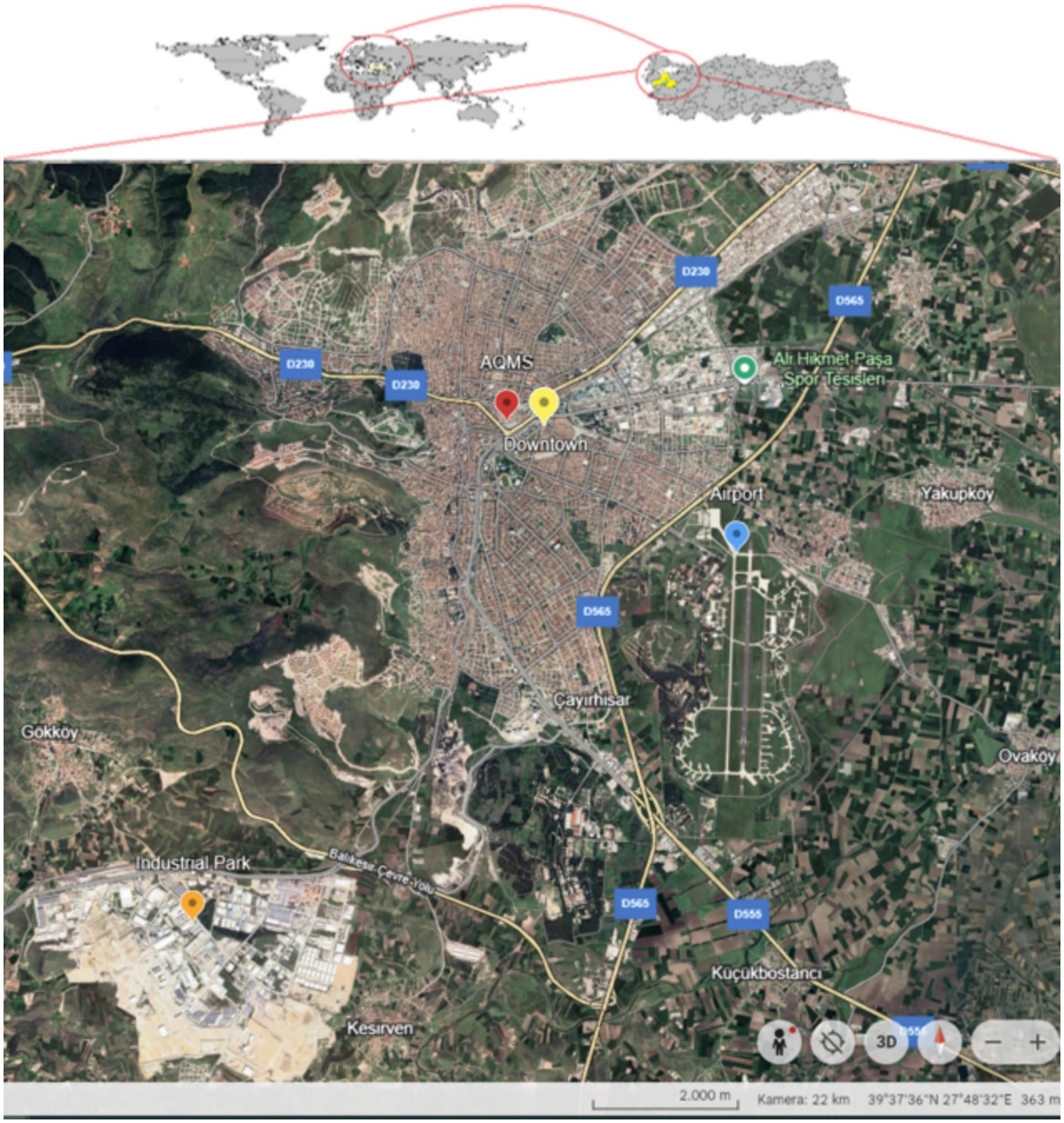

Fig. 1 Aerial view of the study area (© Google Earth, 2025)

on the winter season (December–February). Air pollutant data for PM_{10} (μg m^{-3}) and SO_2 (μg m^{-3}) were obtained from the National Air Quality Monitoring Network (NAQMN, 2024). Air-quality observations for Balıkesir were obtained from a continuous urban background Air Quality Monitoring Station (AQMS) operated by the Turkish Ministry of Environment, Urbanization, and Climate Change (MoEUCC). This station is located near the city center (39° 39′ N, 27° 53′ E; elevation ≈ 140 m a.s.l.) and has provided uninterrupted measurements of PM_{10} and SO_2 since January 2013. The AQMS site is situated within a representative urban basin area influenced by both traffic and domestic heating emissions during winter.

Its location, together with major reference points such as the downtown core, airport, and industrial zone, is shown in Fig. 1 to illustrate the spatial context of the monitoring network. Meteorological data were obtained from the ERA5 reanalysis dataset produced by the European Centre for Medium-Range Weather Forecasts (ECMWF). The data were retrieved through the Copernicus Climate Data Store (ECMWF, 2023) using the official CDS Application Programming Interface (API) in Python. Hourly ERA5 variables, including 2-m air temperature (t2m), surface pressure (sp), dew-point temperature (d2m), and horizontal wind components at 10 m (u10 and v10), were downloaded on a $0.25° \times 0.25°$ spatial grid for the Balıkesir region covering the period 2013–2023. The total wind speed (Ws) was computed as $\sqrt{(u10^2 + v10^2)}$. Relative humidity (RH) was derived from dew-point and air temperature using the standard psychrometric formula. All hourly ERA5 parameters were then aggregated to daily averages to align with the temporal resolution of the AQMS pollutant observations.

Data preparation

Initial preprocessing included removal of duplicates, transformation of time stamps into datetime format, and screening for anomalies. Both PM_{10} and SO_2 datasets were checked for completeness before statistical analysis. Occasional missing values, representing less than 4% of the total daily records between 2013 and 2023, were primarily associated with short-term instrument downtime at the AQMS. Gaps of one to three consecutive days were filled using linear interpolation to preserve temporal continuity, while longer gaps were omitted from the analysis. After this preprocessing step, data completeness reached approximately 96–97% for both pollutants, ensuring that subsequent statistical and trend evaluations were based on reliable and representative time series. Data completeness exceeded 95% across the study period; the small fraction of gaps was screened and excluded from analysis. Outliers were identified via boxplots but preserved for analysis, as they correspond to high-pollution episodes of interest. Descriptive statistics (mean, median, standard deviation, and percentiles) were calculated for all variables to characterize the dataset.

Analytical methods

Exploratory data analysis (EDA) was conducted to characterize pollutant distributions, seasonal cycles, and diurnal patterns, using standard visualization tools and descriptive statistics.

Time series analysis was applied to identify long-term patterns, seasonal periodicities, and short-term fluctuations in pollutant concentrations. The datasets were decomposed into trend, seasonal, and residual components using additive models, enabling clearer identification of interannual and intra-annual variability. Rolling averages and smoothing filters were used to minimize high-frequency noise, while visual inspection of monthly and seasonal means helped detect persistent anomalies and episodic events.

Similar temporal analyses conducted across Türkiye's climatic regions have effectively captured the co-evolution of air pollutants and meteorological factors. Such decomposition techniques are extensively used to separate meteorological fluctuations from emission-induced trends, offering a more accurate interpretation of long-term air quality variability (Eren et al., 2024; Mutlu, 2023).

Pearson correlation coefficients were calculated to examine linear relationships between pollutants and meteorological variables, visualized through correlation matrices and heatmaps. The Pearson correlation coefficient (r) was computed to quantify linear relationships between variables, according to its standard definition (Benesty et al., 2009):

$$r = \frac{\sum (x_i - \bar{x}).(y_i - \bar{y})}{\sqrt{(x_i - \bar{x})^2}.\sqrt{(y_i - \bar{y})^2}}$$

where x_i and y_i are the paired observations, $\bar{x}$ and $\bar{y}$ are their respective means, and Σ denotes summation over n observations. The numerator expresses the covariance between the two variables, while the denominator normalizes this value by their respective standard deviations, yielding a dimensionless coefficient ranging from -1 (perfect negative correlation) to $+1$ (perfect positive correlation).

Correlation results were visualized as color-coded heatmaps to identify dominant relationships and potential multicollinearity among variables. Similar correlation-based approaches were applied by Orak and Özdemir (2021) to link PM_{10} and SO_2

with mobility indicators, and by Katipoğlu et al. (2025) to highlight interrelations among multiple pollutants using Pearson heatmaps for feature analysis (Çıldır & Mutlu, 2022; Katipoğlu et al., 2025; Orak & Ozdemir, 2021).

Inversions were inferred indirectly from high pressure (top 25%), weak winds (<2 m s^{-1}), and elevated pollutant concentrations (Sokhi et al., 2021). Wind component analysis assessed the dispersive role of airflow via scatterplots of concentrations versus U- and V-wind components.

Long-term trends were estimated using the Theil–Sen estimator, a robust non-parametric method resistant to outliers and heteroscedasticity. Long-term trends in daily and annual pollutant concentrations were evaluated using the non-parametric Theil–Sen estimator (Sen, 1968), which computes the median of all pairwise slopes between data points:

$$\beta = \text{median}\,[(xj - xi)/(j - i)], \quad \text{for } 1 \le i < j \le n$$

where β represents the trend slope (change in concentration per unit time), xi and xj are the pollutant concentrations at time indices i and j, respectively, and n is the total number of observations in the time series. The significance of β was tested using the Mann–Kendall statistic (Yue & Wang, 2002). The Theil–Sen method is robust against outliers and non-normal distributions, providing a reliable estimate of monotonic change. This approach, widely adopted in air quality studies, was also utilized by Mutlu (2023) for long-term PM_{10} trend evaluation in the South Marmara Region and by Eren et al. (2024) in a 40-year air quality assessment of Erzurum, both demonstrating its effectiveness for detecting monotonic trends in non-normal environmental datasets (Eren et al., 2024; Mutlu, 2023). Confidence intervals for slopes were computed to determine statistical significance.

To investigate potential regional and long-range transport of air masses, backward trajectory analysis was performed using the Hybrid Single-Particle Lagrangian Integrated Trajectory (HYSPLIT) model developed by NOAA's Air Resources Laboratory (Stein et al., 2015). The model was configured with GDAS 1° meteorological fields, a 48-h backward integration period, and an arrival height of 500 m above ground level at the Balıkesir receptor site (39° 39′ N, 27° 53′ E). Trajectories were computed for representative high-pollution episodes in different seasons to identify dominant transport pathways affecting PM_{10} and SO_2 concentrations. The HYSPLIT framework is widely applied to identify potential source regions and transport pathways of particulate pollutants (Lee et al., 2024; Ma et al., 2021; Saha et al., 2024).

Results

Exploratory data analyses and seasonal variability

Boxplots (Fig. 2) and descriptive statistics (Table 2) show pronounced winter maxima in PM_{10}, with episodic daily values exceeding 400–500 μg m^{-3}. SO_2 exhibits lower central tendencies but occasional high outliers (>100 μg m^{-3}) during the cold season. Table 1 summarises annual sample sizes, means, 95% confidence intervals, and extremes for pollutants and meteorological variables across 2013–2023.

The wider variability and outliers in PM_{10} highlight its episodic nature, while SO_2 shows narrower variability, consistent with gradual improvements in emission controls.

Descriptive statistics (Table 2) summarize central tendencies and variability for pollutants and meteorological parameters.

Annual PM_{10} concentrations fluctuated markedly, with peaks in 2017 and 2021 and a maximum of 576 μg.m^{-3} in 2015, reflecting episodic pollution influenced by both emissions and meteorology.

SO_2 showed interannual variability, peaking at 14.9 μg.m^{-3} in 2021, with occasional extreme values (145 μg.m^{-3} in 2015), likely linked to heating or industrial emissions. These findings point to persistent wintertime challenges despite gradual improvements.

Daily PM_{10} concentrations (Fig. 3) show strong seasonal cycles, with winter peaks exceeding 400 μg.m^{-3} during episodes of increased heating and stagnant meteorology.

Figure 3 shows frequent PM_{10} exceedances both of the National and also the EU daily standard (50 μg m^{-3}), concentrated in winter, consistent with heating emissions and stagnant conditions.

Figure 4 presents the temporal variation of daily SO_2 concentrations over the period 2013–2023. The data reveal notable fluctuations and several pollution

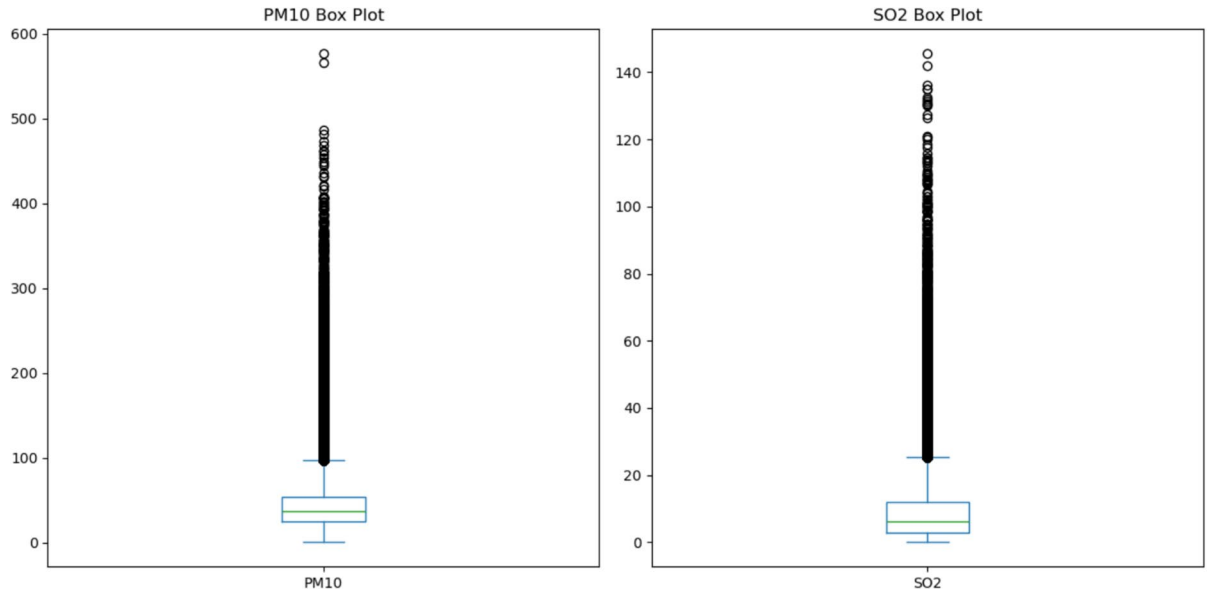

Fig. 2 Box plots of PM_{10} and SO_2 concentrations during winter months (December–February) over the study period (2013–2023)

episodes that highlight the changing emission dynamics across the study years.

Figure 4 shows episodic SO_2 exceedances of both national and EU daily standards (125 μg m^{-3}), most frequent during 2017–2019, followed by a marked decline after 2020 due to improved fuel quality and COVID-19 lockdown effects.

Monthly averages (Fig. 5) confirm winter maxima for both pollutants, driven by heating and reduced dispersion. The lowest PM_{10} levels are observed during the summer months (June through August), when improved atmospheric mixing helps disperse pollutants. SO_2 levels, represented by the orange bars, follow a similar trend, with elevated levels during winter and reduced concentrations in summer. The higher SO_2 levels in winter can be attributed to increased sulfur emissions from heating systems and industrial activities.

Seasonal trends reveal that pollutant concentrations were notably higher during winter months, attributed to increased heating activities and reduced atmospheric dispersion. December and January exhibited peak levels, aligning with seasonal heating demands and stagnant air conditions.

Diurnal patterns (Fig. 6) show PM_{10} peaks in morning and evening commute/heating periods, while SO_2 varies less but increases slightly during the same hours. This reflects its primary source—heating emissions—being less influenced by short-term fluctuations compared to PM_{10}.

Correlations with meteorological variables

Descriptive and correlation-based statistical methods were employed to explore the temporal variability and interrelationships between major air pollutants (PM_{10}, SO_2) and meteorological parameters. These approaches are essential for identifying emission patterns, meteorological influences, and atmospheric stagnation conditions before applying advanced predictive or trend models.

Overall, Pearson correlation analysis remains a key diagnostic tool in air quality research, providing a quantitative foundation for linking pollutant variability with meteorological parameters. When combined with visual methods such as heatmaps, it enhances understanding of atmospheric behavior across spatial and temporal scales and supports trend estimation and model-based forecasting of air pollution episodes.

The winter-only correlation analysis (Fig. 7) provides insights into the interdependencies among pollutants and meteorological parameters in Balıkesir for the period 2013–2023.

A moderate positive correlation ($r = 0.49$) was found between PM_{10} and SO_2, indicating that these pollutants often originate from similar

Table 2 Descriptive statistics of pollutants and meteorological parameters

Parameter	Years	*N*	Mean	95% confidence interval for mean		Minimum	Maximum
				Lower bound	Upper bound		
PM_{10}	2013	8760	48.3	47.5	49.2	2.1	415.9
	2014	8760	45.4	44.6	46.1	1.1	405.4
	2015	8760	44.1	43.3	44.9	3.0	576.3
	2016	8784	42.0	41.4	42.7	1.0	398.2
	2017	8760	55.3	54.2	56.3	2.1	485.9
	2018	8760	45.5	44.7	46.2	1.0	401.9
	2019	8760	34.0	33.5	34.5	0.6	284.2
	2020	8784	43.7	42.8	44.5	1.1	473.3
	2021	8760	62.7	61.8	63.6	4.2	386.0
	2022	8760	53.5	52.7	54.3	3.1	387.3
	2023	8760	43.3	42.8	43.9	2.2	242.9
	Total	96,408	47.1	46.8	47.3	0.6	576.3
SO_2	2013	8760	7.7	7.5	7.9	0.0	108.8
	2014	8760	6.3	6.1	6.4	0.0	110.0
	2015	8760	9.1	8.9	9.3	0.1	145.5
	2016	8784	7.2	7.0	7.4	0.0	120.7
	2017	8760	8.3	8.1	8.6	0.0	136.1
	2018	8760	8.4	8.1	8.6	0.0	131.9
	2019	8760	7.1	7.0	7.3	0.1	77.6
	2020	8784	10.5	10.3	10.7	0.0	106.9
	2021	8760	14.9	14.7	15.1	0.0	134.9
	2022	8760	13.6	13.4	13.8	0.1	98.3
	2023	8760	8.5	8.3	8.6	0.0	43.0
	Total	96,408	9.2	9.2	9.3	0.0	145.5
U-wind speed (10m) (m/s)	2013	8760	−0.3	−0.3	−0.2	−4.6	5.9
	2014	8760	−0.1	−0.1	−0.1	−3.7	8.1
	2015	8760	−0.4	−0.4	−0.4	−4.8	4.8
	2016	8784	−0.2	−0.3	−0.2	−4.6	6.3
	2017	8760	−0.3	−0.3	−0.3	−4.0	5.9
	2018	8760	−0.3	−0.4	−0.3	−5.4	6.5
	2019	8760	−0.4	−0.4	−0.3	−4.5	5.1
	2020	8784	−0.4	−0.4	−0.3	−4.7	5.0
	2021	8760	−0.3	−0.3	−0.3	−4.9	6.2
	2022	8760	−0.5	−0.5	−0.4	−4.4	6.2
	2023	8760	−0.3	−0.3	−0.2	−3.9	5.5
	Total	96,408	−0.3	−0.3	−0.3	−5.4	8.1

Table 2 (continued)

Parameter	Years	*N*	Mean	95% confidence interval for mean		Minimum	Maximum
				Lower bound	Upper bound		
V-wind speed (10m) (m/s)	2013	8760	−1.2	−1.3	−1.1	−7.6	9.3
	2014	8760	−0.9	−1.0	−0.8	−7.6	8.0
	2015	8760	−1.7	−1.8	−1.7	−9.8	11.0
	2016	8784	−1.3	−1.4	−1.3	−8.1	8.7
	2017	8760	−1.4	−1.5	−1.4	−7.9	8.0
	2018	8760	−1.6	−1.6	−1.5	−8.0	8.1
	2019	8760	−1.5	−1.6	−1.5	−8.9	7.8
	2020	8784	−1.7	−1.8	−1.6	−8.1	9.3
	2021	8760	−1.2	−1.3	−1.1	−8.3	8.6
	2022	8760	−1.8	−1.9	−1.8	−7.9	7.2
	2023	8760	−1.2	−1.3	−1.2	−9.7	8.6
	Total	96,408	−1.4	−1.4	−1.4	−9.8	11.0
Temperature (2m) (°C)	2013	8760	15.0	14.8	15.2	−8.5	34.6
	2014	8760	15.6	15.4	15.8	−2.5	37.6
	2015	8760	15.0	14.8	15.1	−7.6	36.8
	2016	8784	15.3	15.1	15.4	−15.7	37.9
	2017	8760	14.6	14.4	14.8	−7.0	38.1
	2018	8760	15.8	15.6	16.0	−3.4	34.8
	2019	8760	15.4	15.2	15.6	−5.2	35.1
	2020	8784	15.2	15.1	15.4	−5.0	35.3
	2021	8760	15.2	15.0	15.4	−7.7	37.4
	2022	8760	14.9	14.7	15.1	−8.8	34.5
	2023	8760	15.7	15.5	15.8	−5.1	40.5
	Total	96,408	15.2	15.2	15.3	−15.7	40.5
Pressure (Pa)	2013	8760	97,734.7	97,722.3	97,747.2	95,870.1	99,612.8
	2014	8760	97,745.7	97,734.6	97,756.8	95,836.8	99,134.1
	2015	8760	97,885.7	97,872.8	97,898.5	96,074.0	99,765.9
	2016	8784	97,835.2	97,822.1	97,848.3	95,599.5	99,918.5
	2017	8760	97,858.7	97,847.7	97,869.7	96,414.3	99,403.6
	2018	8760	97,730.2	97,718.3	97,742.1	95,598.3	99,507.6
	2019	8760	97,753.1	97,742.4	97,763.8	95,864.5	99,336.8
	2020	8784	97,854.8	97,843.0	97,866.6	95,327.3	99,971.1
	2021	8760	97,852.4	97,841.0	97,863.9	95,867.1	99,460.3
	2022	8760	97,876.3	97,864.2	97,888.4	96,264.4	99,704.0
	2023	8760	97,770.2	97,758.8	97,781.7	94,697.0	99,624.1
	Total	96,408	97,808.8	97,805.2	97,812.4	94,697.0	99,971.1

combustion-related sources, such as domestic heating, industrial activities, and traffic emissions that intensify during the cold season.

PM_{10} exhibited weak positive associations with both wind components ($r=0.23$ for U-wind and $r=0.27$ for V-wind), suggesting that horizontal

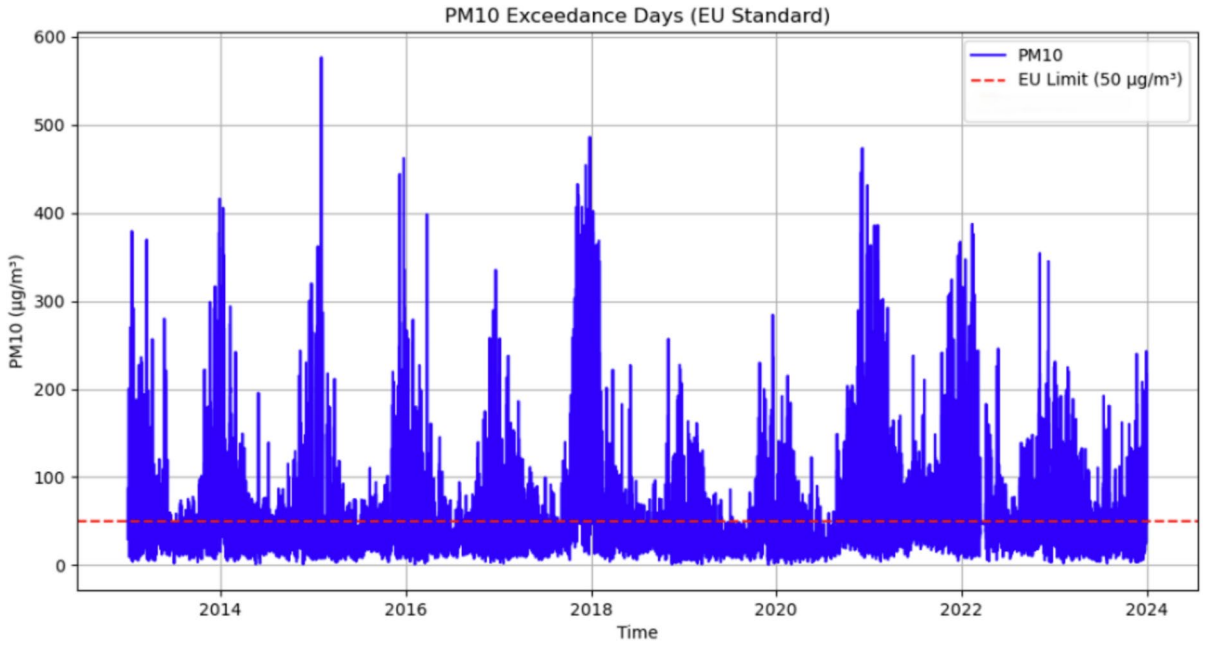

Fig. 3 PM_{10} exceedance days based on the European Union (EU) air quality standard

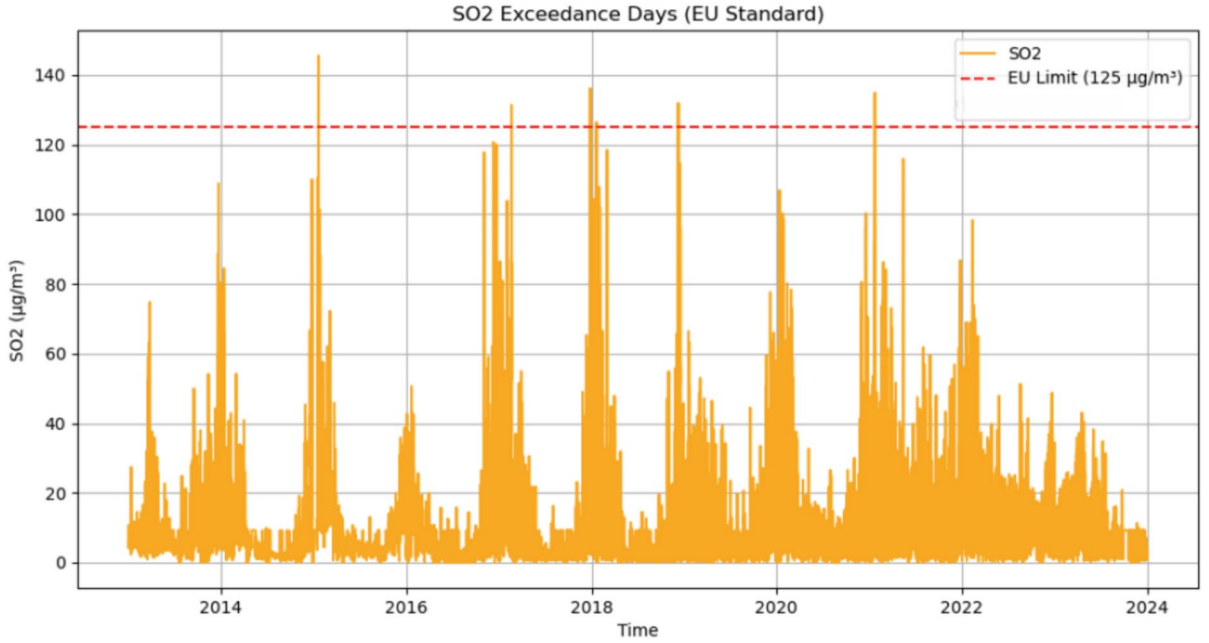

Fig. 4 SO_2 exceedance days based on the European Union (EU) air quality standard

airflows can partially redistribute particulate matter without fully dispersing it under stable winter conditions. Temperature showed a very weak correlation with PM_{10} ($r = 0.04$), reflecting limited direct thermal influence during inversion-dominated periods, while surface pressure displayed a slight positive

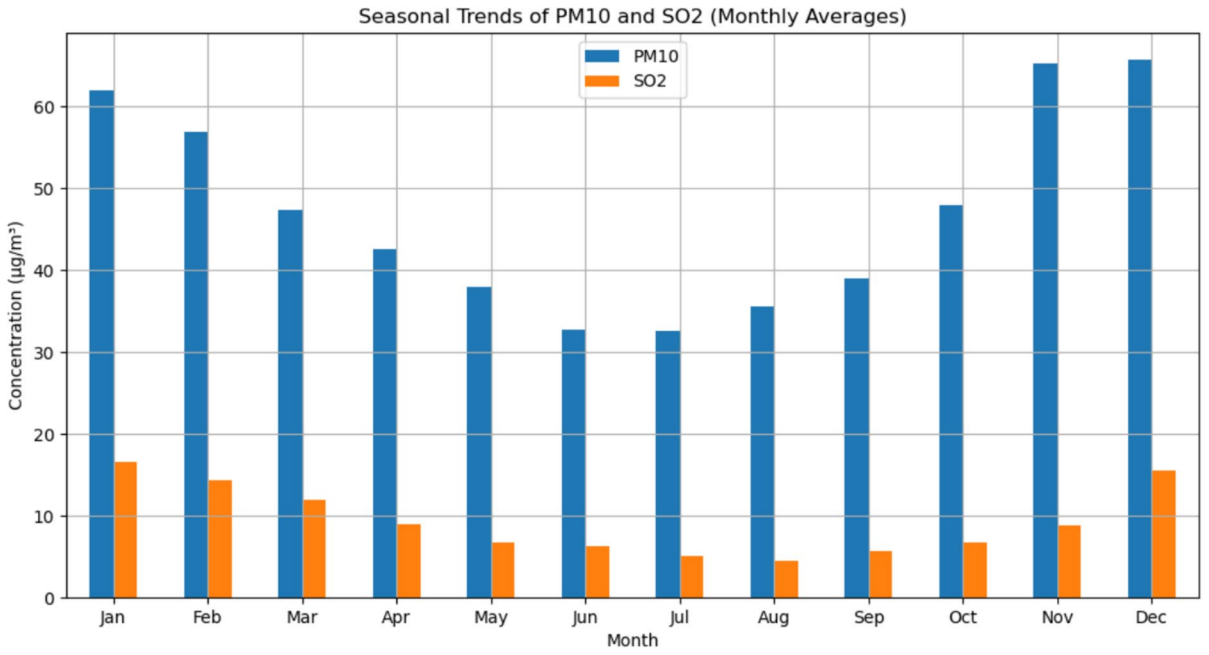

Fig. 5 Seasonal trends in PM_{10} and SO_2 levels as monthly averages

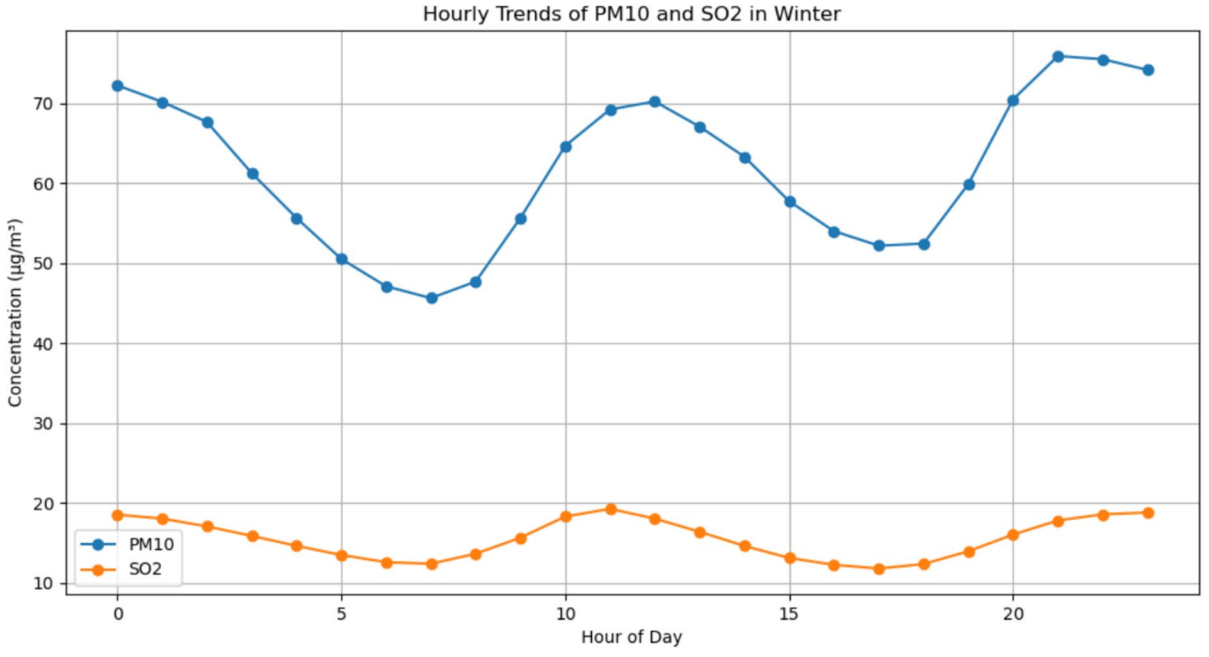

Fig. 6 Hourly trends of PM_{10} and SO_2 concentrations during winter

association ($r = 0.13$), consistent with pollutant accumulation under high-pressure, stagnant weather patterns.

SO_2 also displayed weak or negligible correlations with most meteorological parameters, including temperature ($r = -0.07$) and wind speed components

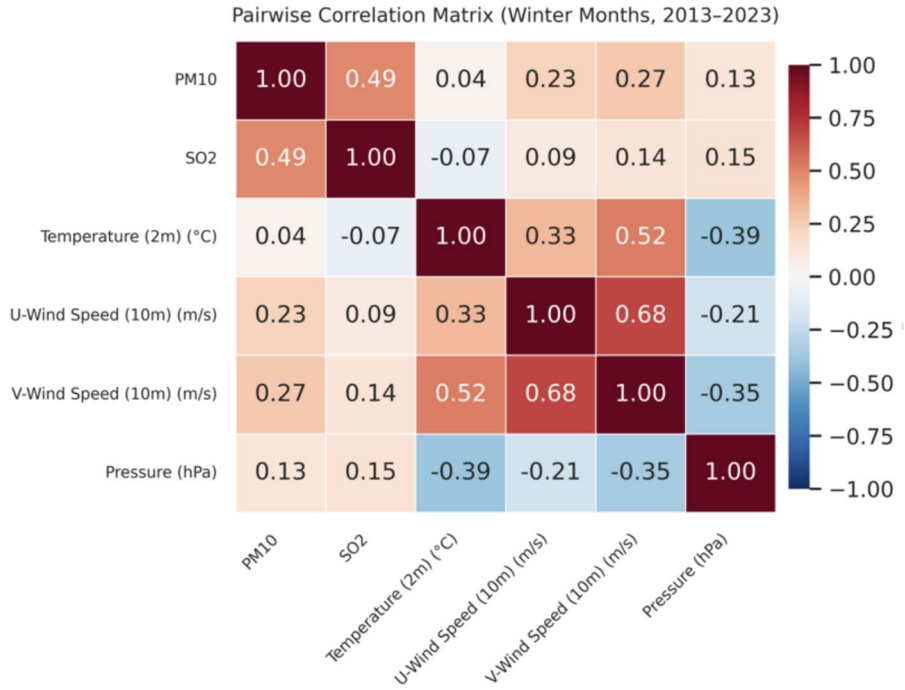

Fig. 7 Correlation matrix for winter months

($r = 0.09$ for U, $r = 0.14$ for V). This pattern implies that SO_2 levels during winter are mainly governed by emission intensity rather than meteorological dispersion, consistent with its origin from continuous combustion sources.

Among meteorological variables themselves, a strong positive relationship ($r = 0.68$) was observed between U- and V-wind components, reflecting the coherence of horizontal wind fields in the region. Temperature correlated positively with both wind components ($r = 0.33$ for U and $r = 0.52$ for V) but negatively with surface pressure ($r = -0.39$), a pattern characteristic of mid-latitude winter systems where colder, high-pressure conditions coincide with reduced atmospheric mixing.

Overall, the correlation matrix confirms that pollutant accumulation in winter is mainly associated with high-pressure and low-dispersion meteorological regimes, while the joint variation of PM_{10} and SO_2 underscores their shared emission dynamics under seasonal heating demand.

Temperature inversions

Temperature inversions were inferred indirectly from conditions of high pressure (top 25% of values), weak horizontal winds (u- and v-wind < 2 m s^{-1}), and concurrent elevated pollutant levels. Average concentrations during inversion days (Fig. 8) reached approximately 85 μg m^{-3} for PM_{10} and slightly above 20 μg m^{-3} for SO_2, compared with about 60 μg m^{-3} and 15 μg m^{-3}, respectively, on non-inversion days.

The mean differences correspond to increases of nearly 40% for PM_{10} and 30% for SO_2 under inversion-prone conditions. These contrasts confirm that pollutant accumulation is consistently higher during high-pressure, low-wind episodes, as reflected by the distinct elevation of both pollutant categories in Fig. 8.

Trend analysis for PM_{10} and SO_2

Long-term pollutant trends were estimated using the Theil–Sen estimator, a robust non-parametric method resistant to outliers and widely applied in air quality studies. The Theil–Sen estimator was applied to identify long-term monotonic trends in PM_{10} and SO_2 concentrations while minimizing the influence of outliers and non-normality in the datasets. This non-parametric method, which calculates the median slope among all possible pairwise comparisons, has been widely recommended for air quality studies due to its robustness against heteroscedasticity and missing data.

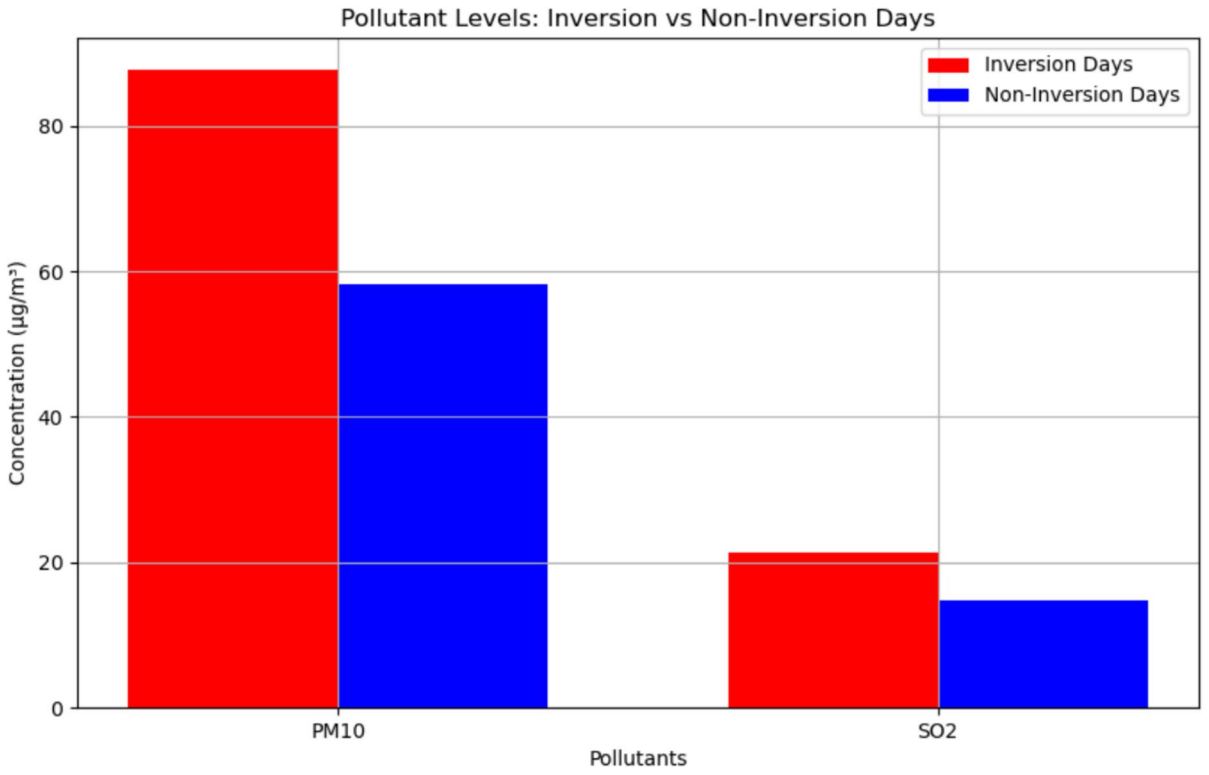

Fig. 8 Pollutants' levels on inversion vs non-inversion days

For PM_{10}, the Theil–Sen estimator indicated a weak, statistically insignificant upward trend of 0.06 $\mu g.m^{-3}$ per year (Fig. 9). Concentrations fluctuated markedly, with annual means ranging from 34 $\mu g.m^{-3}$ in 2019 to 62.7 $\mu g.m^{-3}$ in 2021, exceeding the EU annual limit of 40 $\mu g/m^3$. These variations suggest episodic pollution driven more by short-term factors than by a persistent long-term rise.

Notable anomalies, such as the spike around 2018, significantly deviate from the general trend. These deviations could be attributed to specific meteorological conditions, industrial activities, or unusual events such as wildfires or dust storms. Despite the apparent variability across years, the slight upward trend underscores the importance of examining long-term patterns and their implications for air quality management.

For SO_2, the Theil–Sen estimator indicates a statistically significant positive trend in SO_2 concentrations ($+0.50$ $\mu g\ m^{-3}\ year^{-1}$) over 2013–2023 (Fig. 10). Annual averages fluctuate between 6 $\mu g\ m^{-3}$ and 15 $\mu g\ m^{-3}$, with higher values recorded in the late 2010s. Although the long-term trend remains upward, a short-term dip is visible after 2020, corresponding to the COVID-19 period and reflecting temporary reductions in emissions.

The findings underscore the necessity for targeted air quality management strategies to address the steady increase in SO_2 levels. Future analyses should focus on understanding the contribution of local and regional emission sources, meteorological influences, and the interplay between different pollutants to develop more effective mitigation measures.

The trends for PM_{10} and SO_2 reveal distinct patterns. PM_{10} shows a slight, non-significant upward trend with episodic spikes, indicating localized or seasonal pollution events. In contrast, SO_2 exhibits a significant upward trend, reflecting systemic issues, likely driven by industrial and heating emissions, particularly during winter and under stagnant atmospheric conditions. Together, these findings emphasize the need for targeted mitigation strategies to address SO_2's consistent rise and PM_{10}'s episodic peaks,

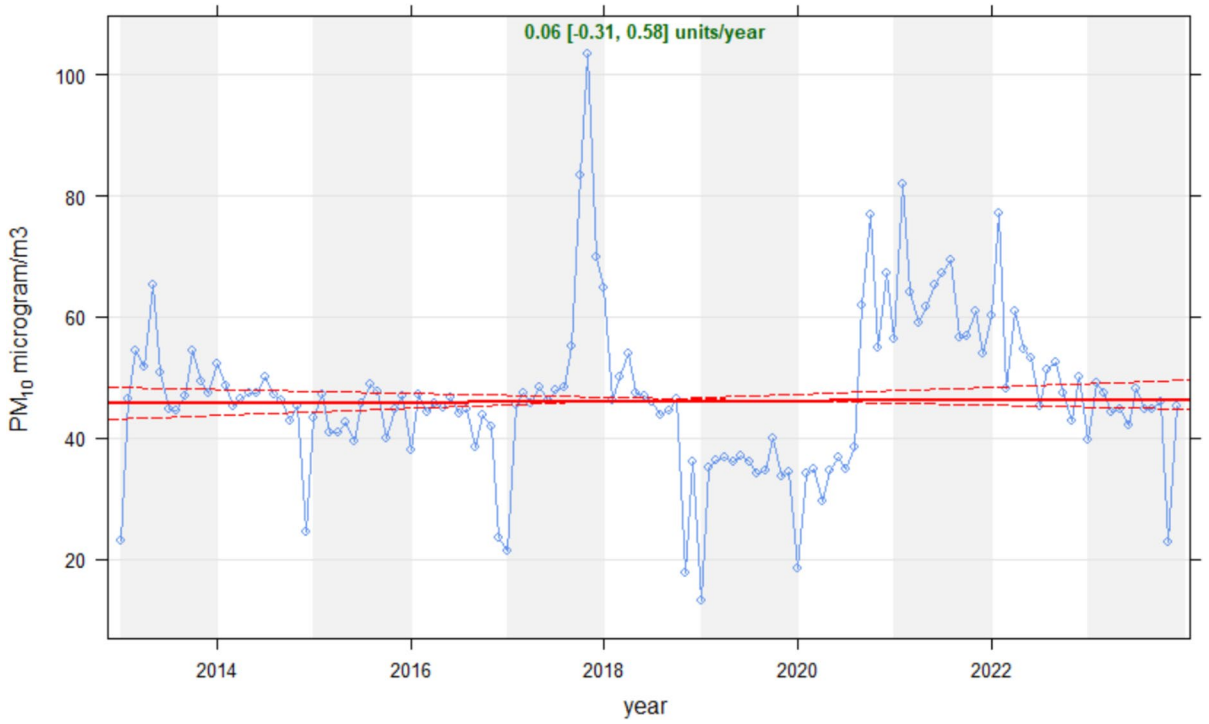

Fig. 9 Theil-Sen trend analysis results for PM_{10} levels

focusing on emission sources and meteorological factors.

Long-range transport episodes

The Hybrid Single-Particle Lagrangian Integrated Trajectory (HYSPLIT) model was used to identify potential source regions and transport pathways affecting PM_{10} and SO_2 levels during high-pollution episodes. The model provides insight into long-range versus local contributions by tracing backward air-mass movements under varying synoptic conditions.

To assess the role of long-range transport in shaping winter pollution, five high-PM_{10} episodes during 2021 were analyzed using 48-h HYSPLIT back trajectories at 500 m above ground level. The selected episodes coincide with observed concentration peaks and provide insight into the regional origin of air masses affecting Balıkesir.

On 21 January 2021 (Fig. 11), backward trajectories showed dominant inflow from Eastern and Southeastern Europe, coinciding with stable winter conditions that limited dispersion. This synoptic pattern indicates that transboundary transport significantly reinforced local accumulation during the episode.

On 3 February 2021 (Fig. 12), air masses originated predominantly from the north–northeast, with more than 70% of trajectories clustered along this pathway. Such persistent inflow highlights the contribution of external air masses in driving elevated concentrations at the receptor site.

On 16 December 2021 (Fig. 13), transport was mainly from the west–southwest, indicating potential contributions from upwind source regions in Southern Europe and the Aegean basin. This westerly inflow demonstrates how maritime and regional air masses can interact with stagnant local conditions to elevate pollution levels.

On 23 December 2021 (Fig. 14), dominant pathways arrived from the southwest and west, consistent with regional-scale advection from the Aegean and Mediterranean sectors. This suggests that emissions transported from these regions, combined with local stagnation, likely contributed to the observed pollution episode.

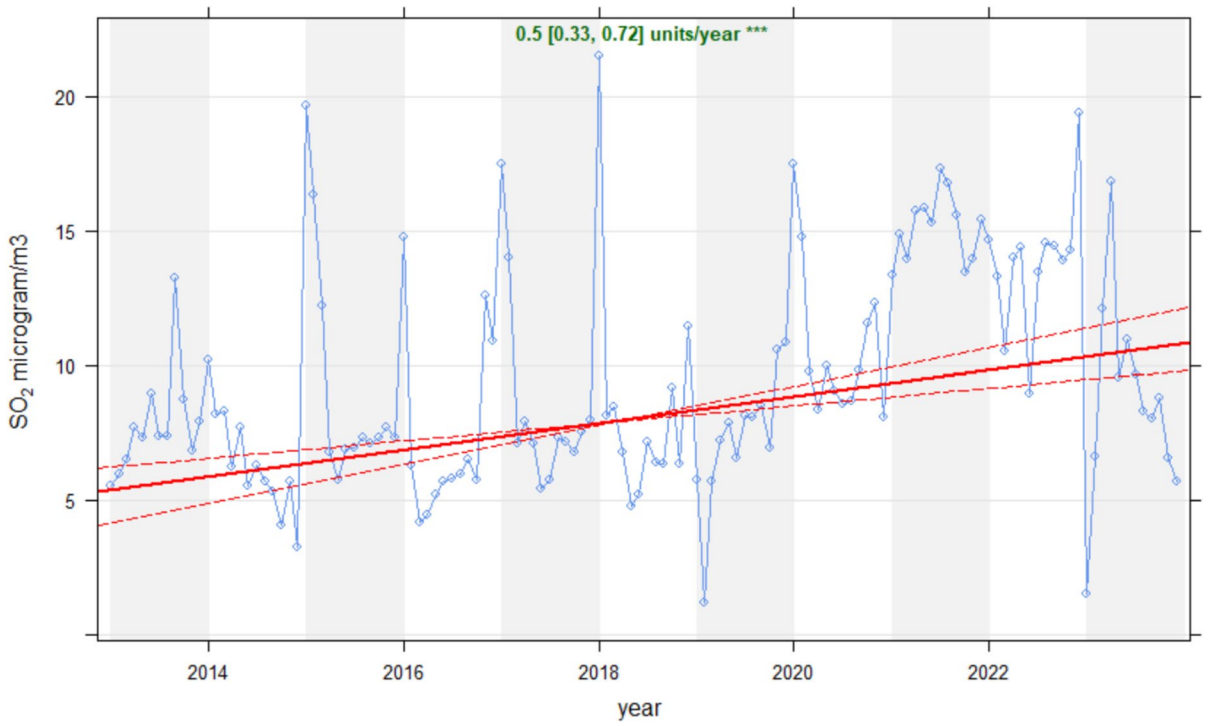

Fig. 10 Theil-Sen trend analysis results for SO_2 levels

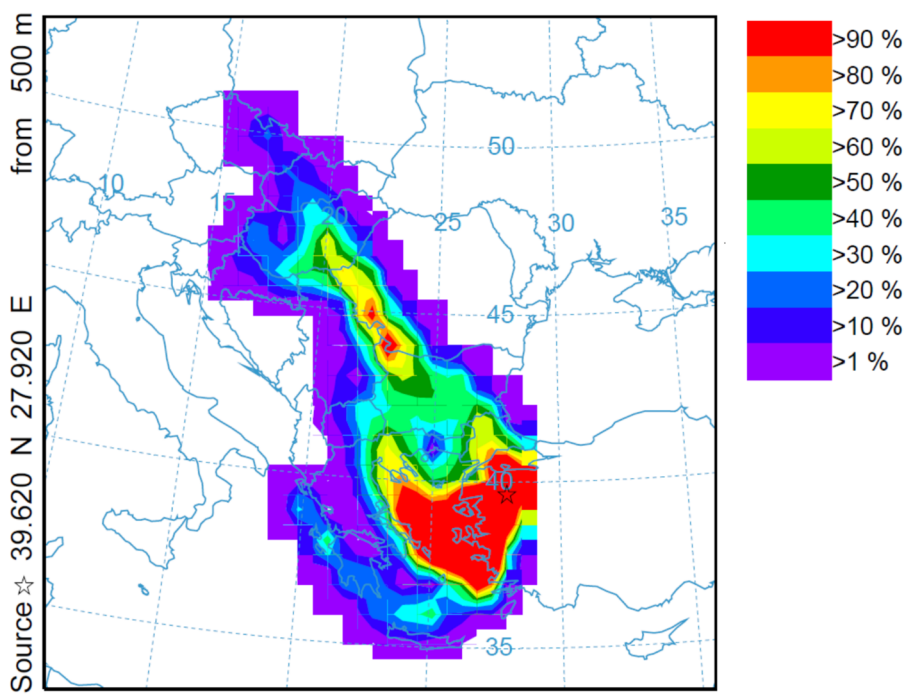

Fig. 11 HYSPLIT 48-h backward trajectories arriving 21 January 2021, 23:00 UTC, at 500 m AGL (trajectory-frequency map, GDAS1, 1.0° × 1.0°)

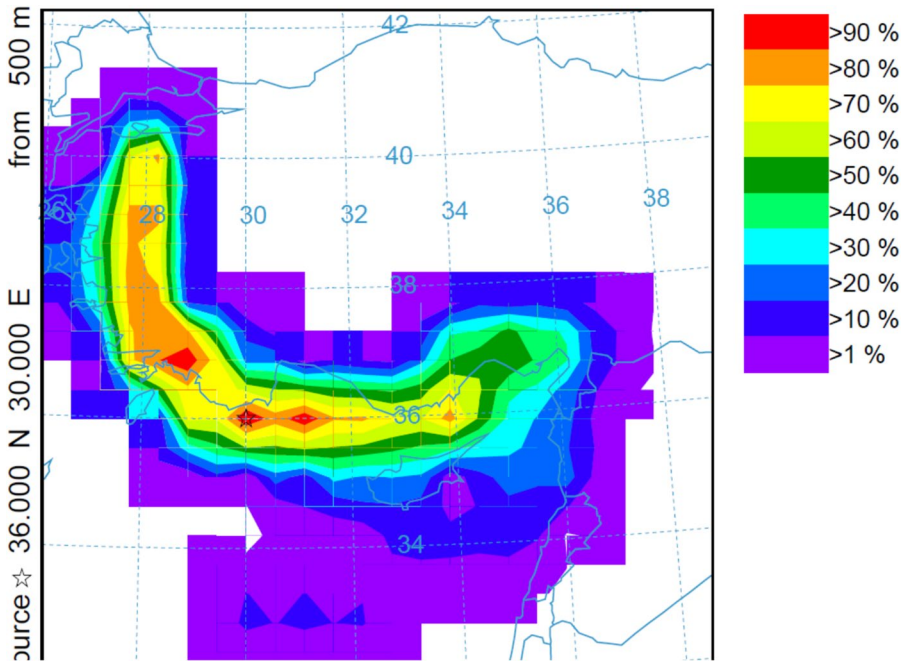

Fig. 12 HYSPLIT 48-h backward trajectories arriving 3 February 2021, 20:00 UTC, at 500 m AGL (trajectory-frequency map, GDAS1, 1.0° × 1.0°)

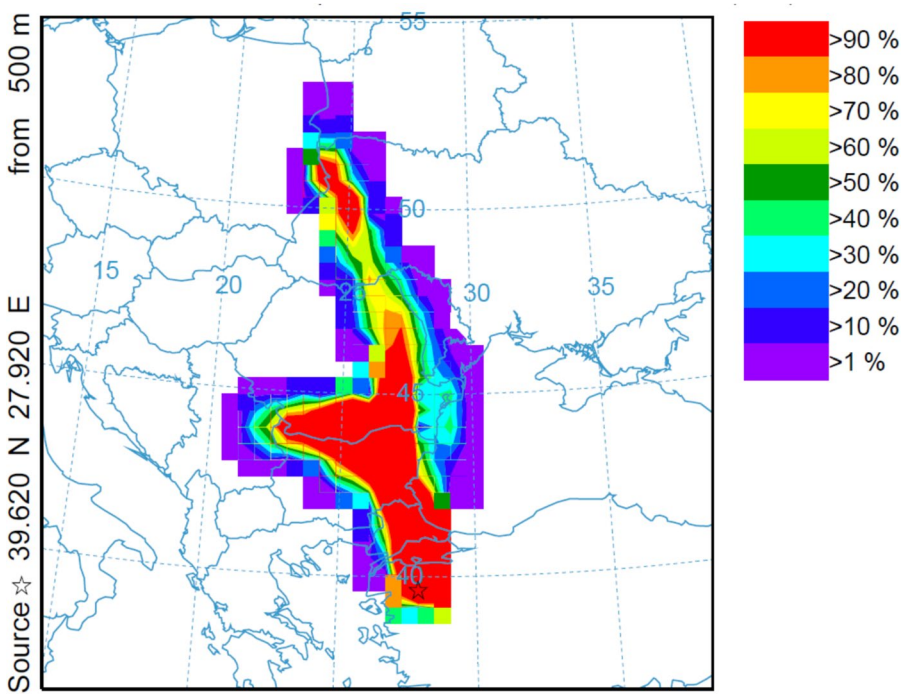

Fig. 13 HYSPLIT 48-h backward trajectories arriving 16 December 2021, 21:00 UTC, at 500 m AGL (trajectory-frequency map, GDAS1, 1.0° × 1.0°)

On 25 December 2021 (Fig. 15), air masses predominantly originated from the northwest, indicating long-range transport from continental Europe. This pathway underscores the significance of transboundary sources in shaping severe winter episodes in Balıkesir.

Taken together, the five case studies (Figs. 11, 12, 13, 14 and 15) confirm that severe winter episodes in

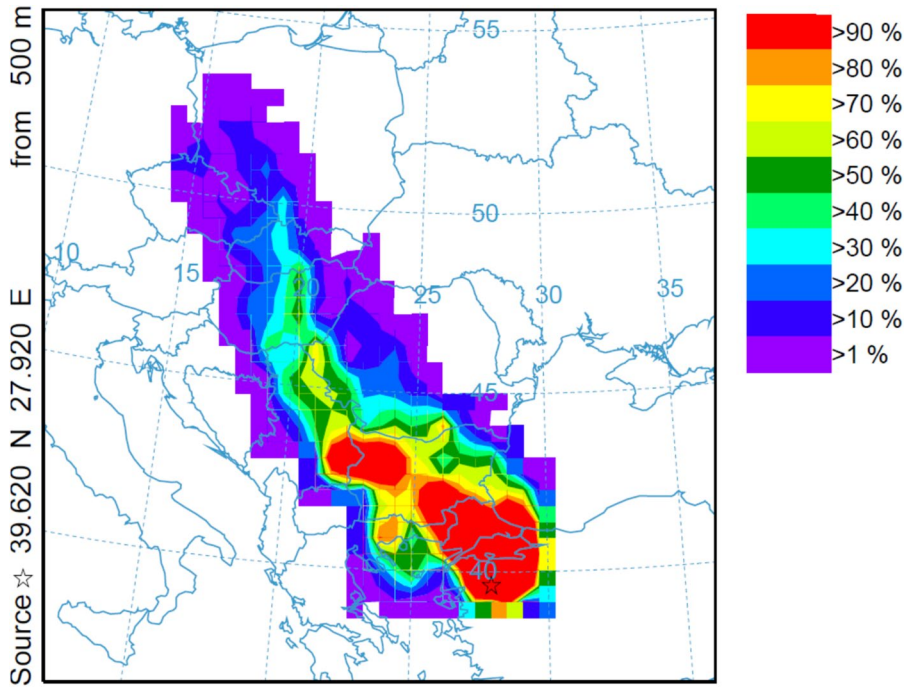

Fig. 14 HYSPLIT 48-h backward trajectories arriving 23 December 2021, 02:00 UTC, at 500 m AGL (trajectory-frequency map, GDAS1, 1.0° × 1.0°)

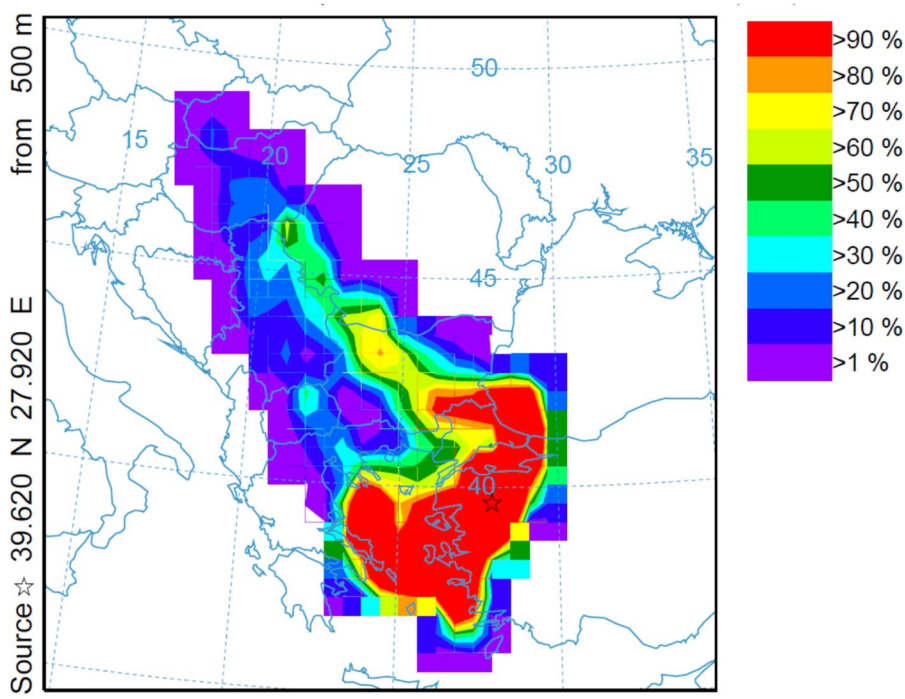

Fig. 15 HYSPLIT 48-h backward trajectories arriving 25 December 2021, 09:00 UTC, at 500 m AGL (trajectory-frequency map, GDAS1, 1.0° × 1.0°)

Balıkesir are not solely the product of local stagnation. Instead, they result from a dual mechanism of unfavorable meteorology and sustained inflows from Eastern, Southeastern, and occasionally Southern and Northwestern Europe.

Discussions

Correlation patterns and meteorological interactions

The seasonal and diurnal behaviour of both pollutants highlights the combined influence of winter meteorology and anthropogenic activities on air quality in Balıkesir. Concentrations of PM_{10} and SO_2 were markedly higher during cold months, driven by increased heating demand, reduced atmospheric dispersion, and temperature inversions that trap pollutants near the surface. Similar episodic winter pollution has been reported in other European and Asian cities where heating demand and meteorological stagnation align (Kumar et al., 2022; Rodrigues et al., 2021; Zhang et al., 2021). The severity and frequency of these exceedance events underline the continuing challenge of managing PM_{10} and SO_2 in urban areas during winter and the necessity for targeted emission-control strategies and public awareness programs to comply with EU air quality standards.

Diurnal trends showed that PM_{10} levels exhibited two distinct daily peaks—morning (07:00–10:00) and evening (18:00–22:00)—attributed to commuting traffic and residential heating, respectively. SO_2 remained relatively stable but increased slightly during the same periods, reflecting the persistence of combustion-related sources. These temporal dynamics confirm that wintertime energy consumption, particularly residential heating, remains a dominant driver of short-term pollution variability across Turkish cities.

Meteorological influences are a decisive factor shaping pollutant accumulation in northwestern Türkiye. Temperature inversions, weak winds, and high-pressure systems together foster stagnant conditions that limit vertical mixing and enhance near-surface pollution. The present results confirm inversion-driven accumulation and support the use of inversion-based early warning indicators for local authorities. These findings align with Guo et al. (2022), who showed that calm winds and strong inversions were the principal meteorological precursors of heavy particulate episodes in the Sichuan Basin (Guo et al., 2022), and with European studies identifying similar stagnation effects (Behera & Gokhale, 2024; Lagmiri & Dahech, 2024). Overall, the correlation structure supports the broader conclusion that winter pollution episodes in mid-latitude cities are primarily controlled by meteorological stagnation and reinforced by seasonal heating demand.

The winter correlation structure (Fig. 7) highlights the joint influence of emission sources and atmospheric processes on air quality in Balıkesir. The moderate positive correlation between PM_{10} and SO_2 ($r = 0.49$) indicates that both pollutants originate primarily from common wintertime combustion sources, including domestic heating and industrial activities. Similar positive linkages between particulate and sulfur species have been reported in other Turkish cities such as Ankara and Zonguldak (Ulutaş et al., 2021, 2022), and in European urban centers dominated by residential heating (Rodrigues et al., 2021; Zhang et al., 2021).

Weak correlations between PM_{10} and temperature ($r = 0.04$) and the slight positive association with pressure ($r = 0.13$) support the interpretation that high-pressure, low-mixing conditions enhance pollutant accumulation, consistent with findings from Guo et al. (2022) and Behera and Gokhale (2024). The positive but limited relationships between PM_{10} and the U- and V-wind components ($r = 0.23$ and 0.27) imply that moderate horizontal transport occurs, yet dispersion remains insufficient under winter stagnation—an effect similarly observed across the South Marmara region (Çıldır & Mutlu, 2022).

For SO_2, the weak associations with meteorological variables—temperature (–0.07), U-wind (0.09), and V-wind (0.14)—suggest that its variability is mainly emission-driven rather than meteorologically controlled. This agrees with studies showing that SO_2 concentrations in Turkish cities respond primarily to heating fuel composition and industrial output rather than synoptic variability (Eren et al., 2024; Mutlu, 2023).

Within the meteorological set, the strong correlation between the U- and V-wind components ($r = 0.68$) demonstrates coherent horizontal flow typical of northwestern Türkiye's basin-like topography. Temperature's positive association with both wind components ($r = 0.33$–0.52) and its negative

correlation with surface pressure ($r = -0.39$) reflects classical winter anticyclonic structures—warm advection with increasing winds and cold, stagnant air under high pressure (Lagmiri & Dahech, 2024).

Taken together, these patterns confirm that winter pollution episodes in Balıkesir are shaped by both source co-variation (PM_{10}–SO_2) and meteorological stagnation (pressure–temperature–wind). The combined analysis underscores the need to consider emission controls and meteorological forecasting simultaneously when developing winter-focused mitigation strategies for northwestern Türkiye.

Long-term trends and trajectory analysis

Trend analyses provide insight into long-term changes in pollutant behaviour. The Theil–Sen results show an insignificant upward trend in PM_{10} but a statistically significant increase in SO_2 (+0.5 μg m^{-3} per year), indicating continued reliance on sulfur-rich fuels or elevated heating demand. These outcomes contrast with declining SO_2 trends observed across much of Europe, suggesting that local energy structures and meteorological conditions still sustain wintertime accumulation in Balıkesir. Comparable studies in Türkiye support this interpretation. Mutlu (2023) identified a steady annual decline of approximately 3.5 μg m^{-3} in PM_{10} across the South Marmara Region from 2007 to 2019, coinciding with expanded natural gas use and cleaner heating practices. Similarly, Eren et al. (2024) reported a sharp decrease in PM and SO_2 concentrations in Erzurum after 2008, attributed to the nationwide transition from coal to natural gas (Eren et al., 2024).

International studies further validate the robustness of the Theil–Sen estimator. Vu et al. (2019) applied the method to meteorologically normalized time series in Beijing, detecting substantial reductions in PM2.5, PM_{10}, and SO_2 linked to regional policy measures (Vu et al., 2019), while Jassim (2018) demonstrated its reliability for long-term PM_{10} analyses under highly variable meteorological conditions in Iraq (Jassim et al., 2018). Collectively, these studies confirm that the Theil–Sen method is a robust tool for detecting structural changes in air quality while distinguishing emission-driven improvements from meteorological noise.

While the overall Theil–Sen analysis indicates a statistically significant long-term increase in SO_2 concentrations (+0.5 μg m^{-3} $year^{-1}$) for 2013–2023, a temporary decline is visible after 2020. This short-term decrease likely reflects the combined influence of cleaner fuel use and the extraordinary conditions associated with the COVID-19 pandemic. Numerous studies have documented that lockdown-related reductions in traffic volume, industrial operations, and energy demand led to notable short-term improvements in air quality worldwide (Akan & Coccia, 2022; Amritha et al., 2024; Han et al., 2024; Saha et al., 2022). Similar effects were observed in Türkiye, where restrictions on mobility and manufacturing activities caused measurable reductions in PM_{10}, NO_2, and SO_2 concentrations (Bugdayci et al., 2023; Kotan & Erener, 2022; Sari & Esen, 2022; Ulutaş et al., 2023). Therefore, the post-2020 decline in SO_2 exceedances in Balıkesir likely represents a transient response to both regulatory progress and pandemic-related emission reductions within an overall upward long-term trend.

Transport analyses further illustrate the interplay between local and regional processes. HYSPLIT backward trajectories show that severe winter episodes in Balıkesir result from the combined effect of stagnant local meteorology and sustained inflows from Eastern, Southeastern, and occasionally Southern or Northwestern Europe. Similar findings were reported by Ma et al. (2021), Lee et al. (2024), and Kavitha et al. (2023), who identified the dual influence of regional advection and weak dispersion on winter air quality (Kavitha et al., 2023; Lee et al., 2024; Ma et al., 2021). In Türkiye, Dogan and Atbinici (2022) linked Saharan dust incursions to spring–autumn PM_{10} peaks, whereas SO_2 remained dominated by local heating sources (Dogan & Atbinici, 2022). Çıldır and Mutlu (2022) confirmed that Balıkesir's episodes coincide with weak ventilation and shallow boundary layers (Çıldır & Mutlu, 2022), while Saha et al. (2024) showed how dispersion efficiency above 2000 m AGL improves markedly in summer, reducing pollutant retention (Saha et al., 2024).

Overall, HYSPLIT consistently demonstrates that PM_{10} variability is shaped by regional advection and meteorological stagnation, whereas SO_2 changes are mainly local in origin. These findings underscore the importance of meteorology, emission patterns, and transboundary influence in shaping air quality dynamics across northwestern Türkiye.

Implications and policy relevance

Effective mitigation requires integrating local and regional perspectives: improving residential heating efficiency, tightening industrial emission controls, and strengthening early-warning systems for inversion-prone days. Continuous cooperation with neighbouring provinces and transboundary partners will be essential to address transported PM, while sustained adoption of cleaner fuels will help mitigate SO_2 accumulation. Future research should combine trajectory analysis with emission inventories, satellite-based vertical profiles, and machine-learning models to enhance predictive capacity and support science-based air quality policy.

Conclusions

This study provides a decade-long evaluation of PM_{10} and SO_2 air pollution in Balıkesir (2013–2023), integrating statistical trend analysis, seasonal and diurnal patterns, meteorological influences, and transboundary transport diagnostics. The results demonstrate that wintertime heating, traffic emissions, and stagnant meteorological conditions are the dominant factors controlling high pollution levels, with temperature inversions exerting a particularly critical influence on surface accumulation.

The Pearson correlation analysis further confirmed that PM_{10} and SO_2 are moderately associated ($r = 0.49$), reflecting their common origin from combustion-related sources. Weak but consistent correlations between pollutants and meteorological variables, particularly temperature (negative) and surface pressure (positive), revealed that stagnant high-pressure conditions and weak horizontal winds enhance pollutant retention during winter episodes.

Trend analysis revealed that PM_{10} exhibits strong episodic variability without a statistically significant long-term trend, whereas SO_2 shows a clear and significant upward tendency, indicating persistent sulfur emissions during cold seasons. HYSPLIT trajectory analysis confirmed that severe winter episodes are shaped by both local stagnation and long-range inflow, predominantly from Eastern and Southeastern Europe.

These outcomes highlight that while local emission controls remain essential, they are insufficient to ensure sustainable air quality improvements. A comprehensive strategy combining stricter seasonal fuel regulations, inversion-based early-warning systems, and enhanced regional cooperation is required to mitigate the dual impacts of local and transported pollution.

Future research should expand the analytical framework by incorporating additional pollutants (e.g., NO_x, O_3, and $PM_{2.5}$), vertical inversion parameters from radiosonde or satellite profiles, and machine-learning-based forecasting tools. Such integrated approaches will further strengthen the understanding of emission–meteorology–transport interactions and support evidence-based policymaking for cleaner air across northwestern Türkiye.

Author contributions The author conceived the study, developed the theoretical framework, performed all data analyses and model applications, and wrote and edited the manuscript.

Funding The author gratefully acknowledges the financial support provided by the Division of Scientific Research Projects of Balıkesir University under Project No: BAP.2025/146. This funding was instrumental in enabling the collection, processing, and analysis of data, as well as the development of the models employed in the study.

Data availability The data used in this study are available from the author upon reasonable request. Air pollutant and meteorological data were obtained from official, real-time, and continuously monitored stations. These datasets include high-resolution measurements that were essential for the analyses conducted in this research.

Declarations

Ethics approval This study used publicly available or authorized data and did not involve humans or animals. Clinical trial number is not applicable.

Consent to participate The author confirms their consent to participate in this study and to contribute to the research and publication process.

Consent for publication The author provides their consent for the publication of this work and confirms agreement with the final version of the manuscript.

Competing interests The authors declare no competing interests.

References

Aas, W., Fagerli, H., Alastuey, A., Cavalli, F., Degorska, A., Feigenspan, S., Brenna, H., Gliss, J., Heinesen, D., Hueglin, C., Holubová, A., Jaffrezo, J. L., Mortier, A., Murovec, M., Putaud, J. P., Rüdiger, J., Simpson, D., Solberg, S., Tsyro, S., … Yttri, K. E. (2024). Trends in air pollution in Europe, 2000-2019. *Aerosol and Air Quality Research*. https://doi.org/10.4209/aaqr.230237

Akan, A. P., & Coccia, M. (2022). Changes of air pollution between countries because of lockdowns to face COVID-19 pandemic. *Applied Sciences, 12*(24), 12806.

Amritha, S., Patel, V., & Kuttippurath, J. (2024). The COVID-19 lockdown induced changes of SO2 pollution in its human-made global hotspots. *Global Transitions, 6*, 152–163.

Araujo, L. N., Belotti, J. T., Alves, T. A., Tadano, Y. D., & Siqueira, H. (2020). Ensemble method based on artificial neural networks to estimate air pollution health risks. *Environmental Modelling & Software*. https://doi.org/10.1016/j.envsoft.2019.104567

BCAAP. (2024). *Balıkesir Clean Air Action Plan (THEP 2020–2024)*. Republic of Turkey, Ministry of Environment and Urbanization, Balikesir Environment and Urbanization Provincial Directorate. Retrieved December 17, 2024, from https://webdosya.csb.gov.tr/db/balikesir/menu/thep-son-26_20200310014921.pdf

Behera, N., & Gokhale, S. (2024). Understanding meteorological factors influencing heavy air pollution in Guwahati, India. *Atmospheric Pollution Research*, 102337. https://doi.org/10.1016/j.apr.2024.102337

Benesty, J., Chen, J., Huang, Y., & Cohen, I. (2009). Pearson correlation coefficient. In *Noise reduction in speech processing* (pp. 1–4). Springer. https://doi.org/10.1007/978-3-642-00296-0_5

Bhardwaj, P., Ki, S. J., Kim, Y. H., Woo, J. H., Song, C. K., Park, S. Y., & Song, C. H. (2019). Recent changes of trans-boundary air pollution over the Yellow Sea: Implications for future air quality in South Korea. *Environmental Pollution, 247*, 401–409. https://doi.org/10.1016/j.envpol.2019.01.048

Bodor, Z., Bodor, K., Keresztesi, Á., & Szép, R. (2020). Major air pollutants seasonal variation analysis and long-range transport of PM10 in an urban environment with specific climate condition in Transylvania (Romania). *Environmental Science and Pollution Research, 27*(30), 38181–38199. https://doi.org/10.1007/s11356-020-09838-2

Bugdayci, I., Ugurlu, O., & Kunt, F. (2023). Spatial analysis of SO2, PM10, CO, NO2, and O3 pollutants: The case of Konya province, Turkey. *Atmosphere, 14*(3), Article 462. https://doi.org/10.3390/atmos14030462

Cichowicz, R., & Dobrzański, M. (2021). 3D spatial analysis of particulate matter (PM10, PM2.5 and PM1.0) and gaseous pollutants (H2S, SO2 and VOC) in urban areas surrounding a large heat and power plant. *Energies, 14*(14), Article 4070. https://doi.org/10.3390/en14144070

Çıldır, İ, & Mutlu, A. (2022). Balıkesir şehir merkezinde hava kirliliği seviyelerinin zamansal ve mekansal analizleri. *Journal of Advanced Research in Natural and Applied Sciences, 8*(2), 246–266.

Dogan, R. T., & Atbinici, M. (2022). Temporal and spatial analysis of PM10 and SO2 concentration with the use of GIS in southeastern Anatolia region cities of Turkey (2010–2020). https://doi.org/10.15666/aeer/2005_40794093

ECMWF. (2023). *ERA5 hourly data on pressure levels from 1940 to present* https://doi.org/10.24381/cds.bd0915c6

Eren, Z., Şahin, Ü., & Toy, S. (2024). The evaluation of forty years of air quality and trend of air pollutants in Erzurum City. *International Journal of Environmental Science and Technology, 21*(15), 9425–9446.

EU. (18.09.2015). *Directive 2008/50/EC of the European Parliament and of the Council of 21 May 2008 on ambient air quality and cleaner air for Europe*. EYR-Lex. Retrieved October 20, 2025, from http://data.europa.eu/eli/dir/2008/50/oj

Guo, Q., Wu, D., Yu, C., Wang, T., Ji, M., & Wang, X. (2022). Impacts of meteorological parameters on the occurrence of air pollution episodes in the Sichuan basin. *Journal of Environmental Sciences (China), 114*, 308–321. https://doi.org/10.1016/j.jes.2021.09.006

Han, H., Hasnain, A., Bhatti, U. A., Yue, Y., He, Y., Wei, G., ur Rahman, W., & Akhter, Z. H. (2024). Assessing the spatio-temporal impact of the COVID-19 pandemic lockdown on air quality in Jiangsu province, China. *Environment, Development and Sustainability*, 1–21. https://doi.org/10.1007/s10668-024-04914-w

HKDY. (2008). *Hava Kalitesi Değerlendirme ve Yönetimi Yönetmeliği (HKDY)*. TC Resmi Gazete. Retrieved October 20, 2025, from https://www.resmigazete.gov.tr/eskiler/2008/06/20080606-6.htm

Huang, Y., Lei, C., Liu, C. H., Perez, P., Forehead, H., Kong, S., & Zhou, J. L. (2021). A review of strategies for mitigating roadside air pollution in urban street canyons. *Environmental Pollution, 280*, Article 116971. https://doi.org/10.1016/j.envpol.2021.116971

Imam, M., Adam, S., Dev, S., & Nesa, N. (2024). Air quality monitoring using statistical learning models for sustainable environment. *Intelligent Systems with Applications, 22*, Article 200333. https://doi.org/10.1016/j.iswa.2024.200333

Iqbal, M., Susilo, B., & Hizbaron, D. R. (2025). How local pollution and transboundary air pollution impact air quality in Jakarta? *Papers in Applied Geography, 11*(1), 49–62. https://doi.org/10.1080/23754931.2024.2399626

Jassim, M. S., Coskuner, G., & Munir, S. (2018). Temporal analysis of air pollution and its relationship with meteorological parameters in Bahrain, 2006–2012. *Arabian Journal of Geosciences, 11*(3), 62. https://doi.org/10.1007/s12517-018-3403-z

Javed, Z., Bilal, M., Qiu, Z., Li, G., Sandhu, O., Mehmood, K., Wang, Y., Ali, M. A., Liu, C., & Wang, Y. (2022). Spatiotemporal characterization of aerosols and trace gases over the Yangtze River Delta region, China: Impact of trans-boundary pollution and meteorology. *Environmental Sciences Europe, 34*(1), 86. https://doi.org/10.1186/s12302-022-00668-2

Kalantari, E., Gholami, H., Malakooti, H., Eftekhari, M., Saneei, P., Esfandiarpour, D., Moosavi, V., & Nafarzadegan, A. R. (2024). Evaluating traditional versus ensemble machine learning methods for predicting missing

data of daily PM10 concentration. *Atmospheric Pollution Research, 15*(5), Article 102063. https://doi.org/10.1016/j.apr.2024.102063

Katipoğlu, O. M., Elshaboury, N., Kartal, V., Ertugay, N., Kilinc, H. C., Şenocak, S., & Pande, C. B. (2025). Application of time series methodologies for robust forecasting of atmospheric pollutant concentrations: PM10, SO2, NO2, NOx, and O3 in an urban environment. *Environmental Quality Management, 35*(2), Article e70206. https://doi.org/10.1002/tqem.70206

Kavitha, C., Raju Dharma, A., Kumar, S., & Chilaka Rao, M. (2023). Air quality concentration, transport/dispersion and pathways of particulate matter during community celebration of Diwali days over Visakhapatnam city. *Research Journal of Chemistry and Environment*, *27*, 8. https://doi.org/10.25303/2708rjce022034

Khaslan, Z., Nadzir, M. S. M., Johar, H., Siqi, Z., Sulong, N. A., Mohamed, F., Majumdar, S., Suris, F. N. A., Hawari, N. S. S. L., Borah, J., Gee, M. O. C., Wahab, M. I. A., Abu Bakar, M. A., Ariff, N. M., Japeri, A. Z. U. M., Nor, M. F. F. M., Rabuan, U., Ali, S. H. M., Murugan, B., & Cayetano, M. G. (2024). Utilizing a low-cost air quality sensor: Assessing air pollutant concentrations and risks using low-cost sensors in Selangor, Malaysia. *Water, Air, and Soil Pollution, 235*(4), Article 229. https://doi.org/10.1007/s11270-024-07012-9

Kotan, B., & Erener, A. (2022). Seasonal analysis and mapping of air pollution (PM10 and SO2) during COVID-19 lockdown in Kocaeli (Türkiye). *International Journal of Engineering and Geosciences, 8*(2), 173–187. https://doi.org/10.26833/ijeg.1111699

Kumar, P., Singh, A. B., & Singh, R. (2022). Comprehensive health risk assessment of microbial indoor air quality in microenvironments. *PLoS ONE, 17*(2), Article e0264226. https://doi.org/10.1371/journal.pone.0264226

Lagmiri, S., & Dahech, S. (2024). Temperature inversion and particulate matter concentration in the low troposphere of Cergy-Pontoise (Parisian Region). *Atmosphere, 15*(3), 349. https://doi.org/10.3390/atmos15030349

Lee, S.-J., Song, C.-K., & Choi, S.-D. (2024). Past and recent changes in the pollution characteristics of PM10 and SO2 in the largest industrial city in South Korea. *Atmospheric Environment, 319*, Article 120310. https://doi.org/10.1016/j.atmosenv.2023.120310

Lembo, R., Landoni, G., Cianfanelli, L., & Frontera, A. (2021). Air pollutants and SARS-CoV-2 in 33 European countries. *Acta Biomedica, 92*(1), Article e2021166. https://doi.org/10.23750/abm.v92i1.11155

Ma, Y., Wang, M., Wang, S., Wang, Y., Feng, L., & Wu, K. (2021). Air pollutant emission characteristics and HYSPLIT model analysis during heating period in Shenyang, China. *Environmental Monitoring and Assessment, 193*(1), Article 9.

Mai, K. (2024). Influence of air quality on respiratory health in urban areas in Japan. *Global Journal of Health Science, 9*(2), 49–58. https://doi.org/10.47604/gjhs.2572

Masoud, A. A. (2023). Spatio-temporal patterns and trends of the air pollution integrating MERRA-2 and in situ air quality data over Egypt (2013–2021). *Air Quality, Atmosphere & Health, 16*(8), 1543–1570.

Mutlu, A. (2023). Spatial and temporal analyses of airborne particulate matter in South Marmara Region of Turkey. *International Journal of Environment and Pollution, 72*(1), 1–16. https://doi.org/10.1504/IJEP.2023.135413

NAQMN. (2024). *National Air Quality Monitoring Network*. Ministry of Environment, Urbanisation and Climate Change. Retrieved November 21, 2024, from https://sim.csb.gov.tr/Services/AirQuality

Opeoluwa Oluwanifemi, A., Tolulope, O., Evangel Chinyere, A., Femi, O., Jane Osareme, O., & Onyeka Henry, D. (2024). Air quality and public health: A review of urban pollution sources and mitigation measures. *Engineering Science & Technology Journal, 5*(2), 259–271. https://doi.org/10.51594/estj.v5i2.751

Orak, N. H., & Ozdemir, O. (2021). The impacts of COVID-19 lockdown on PM10 and SO2 concentrations and association with human mobility across Turkey. *Environmental Research, 197*, Article 111018. https://doi.org/10.1016/j.envres.2021.111018

Park, I.-S., Kim, H.-K., Song, C.-K., Jang, Y.-W., Kim, S.-H., Cho, C.-R., Owen, J. S., Kim, C.-H., Chung, K.-W., & Park, M.-S. (2019). Meteorological characteristics and assessment of the effect of local emissions during high PM10 concentration in the Seoul Metropolitan Area. *Asian Journal of Atmospheric Environment, 13*(2), 117–135. https://doi.org/10.5572/ajae.2019.13.2.117

Robotto, A., Barbero, S., Bracco, P., Cremonini, R., Ravina, M., & Brizio, E. (2022). Improving air quality standards in Europe: Comparative analysis of regional differences, with a focus on Northern Italy. *Atmosphere, 13*(5), 642. https://doi.org/10.3390/atmos13050642

Rodrigues, V., Gama, C., Ascenso, A., Oliveira, K., Coelho, S., Monteiro, A., Hayes, E., & Lopes, M. (2021). Assessing air pollution in European cities to support a citizen centered approach to air quality management. *Science of the Total Environment, 799*, Article 149311. https://doi.org/10.1016/j.scitotenv.2021.149311

Saha, L., Kumar, A., Kumar, S., Korstad, J., Srivastava, S., & Bauddh, K. (2022). The impact of the COVID-19 lockdown on global air quality: A review. *Environmental Sustainability, 5*(1), 5–23. https://doi.org/10.1007/s42398-021-00213-6

Saha, S., Bhattacharjee, S., Bera, B., & Haque, E. (2024). Drivers of high concentration and dispersal of PM10 and PM2.5 in the eastern part of Chhota Nagpur plateau, India, investigated through HYSPLIT model and improvement of environmental health quality. *Environmental Quality Management, 34*(1), Article e22299. https://doi.org/10.1002/tqem.22299

Sari, M. F., & Esen, F. (2022). Effect of COVID-19 on PM10 and SO2 concentrations in Turkey. *Environmental Forensics, 23*(5–6), 445–454. https://doi.org/10.1080/15275922.2021.1907818

Sen, P. K. (1968). Estimates of the regression coefficient based on Kendall's tau. *Journal of the American statistical association, 63*(324), 1379–1389. https://doi.org/10.1080/01621459.1968.10480934

Sicard, P., Agathokleous, E., De Marco, A., Paoletti, E., & Calatayud, V. (2021). Urban population exposure to air pollution in Europe over the last decades. *Environmental*

Sciences Europe, 33(1), 28. https://doi.org/10.1186/s12302-020-00450-2

Sokhi, R. S., Moussiopoulos, N., Baklanov, A., Bartzis, J., Coll, I., Finardi, S., Friedrich, R., Geels, C., Grönholm, T., & Halenka, T. (2021). Advances in air quality research–current and emerging challenges. *Atmospheric Chemistry and Physics Discussions, 2021*, 1–133. https://doi.org/10.5194/acp-22-4615-2022

Stein, A. F., Draxler, R. R., Rolph, G. D., Stunder, B. J., Cohen, M. D., & Ngan, F. (2015). NOAA's HYSPLIT atmospheric transport and dispersion modeling system. *Bulletin of the American Meteorological Society, 96*(12), 2059–2077. https://doi.org/10.1175/BAMS-D-14-00110.1

Tang, D., Zhan, Y., & Yang, F. (2024). A review of machine learning for modeling air quality: Overlooked but important issues. *Atmospheric Research, 300*, Article 107261. https://doi.org/10.1016/j.atmosres.2024.107261

Ulutaş, K., Abujayyab, S. K., & Amr, S. A. (2021). Evaluation of the major air pollutants levels and its interactions with meteorological parameters in Ankara. *Mühendislik Bilimleri ve Tasarım Dergisi, 9*(4), 1284–1295.

Ulutaş, K., Abujayyab, S. K., Amr, S. S. A., Alkarkhi, A. F., & Duman, S. (2023). The effect of air quality parameters on new COVID-19 cases between two different climatic and geographical regions in Turkey. *Theoretical and Applied Climatology, 152*(1–2), Article 801. https://doi.org/10.1007/s00704-023-04420-5

Ulutaş, K., Alkarkhi, A. F., Abujayyab, S. K., & Abu Amr, S. (2022). Multivariate analysis for air contamination and meteorological parameters in Zonguldak, Turkey. *Jordan Journal of Civil Engineering, 16*(4). http://hdl.handle.net/123456789/28499

van Pinxteren, D., Mothes, F., Spindler, G., Fomba, K. W., & Herrmann, H. (2019). Trans-boundary PM10: Quantifying impact and sources during winter 2016/17 in eastern Germany. *Atmospheric Environment, 200*, 119–130. https://doi.org/10.1016/j.atmosenv.2018.11.061

Vu, T., Shi, Z., & Harrison, R. M. (2019). Clean air action and air quality trends in Beijing Megacity. *Geophysical Research Abstracts, 21*, 1.

WHO. (2021). *WHO global air quality guidelines: Particulate matter (PM2. 5 and PM10), ozone, nitrogen dioxide, sulfur dioxide and carbon monoxide (Licence: CC-BY-NC-SA 3.0 IGO. ed.)*. World Health Organization.

Yang, J. B., & Shao, M. (2021). Impacts of extreme air pollution meteorology on air quality in China. *Journal of Geophysical Research: Atmospheres*. https://doi.org/10.1029/2020JD033210

Yue, S., & Wang, C. Y. (2002). Applicability of prewhitening to eliminate the influence of serial correlation on the Mann-Kendall test. *Water Resources Research, 38*(6), 4-1–4-7. https://doi.org/10.1029/2001WR000861

Zhang, Y., Chen, X., Yu, S., Wang, L., Li, Z., Li, M., Liu, W., Li, P., Rosenfeld, D., & Seinfeld, J. H. (2021). City-level air quality improvement in the Beijing-Tianjin-Hebei region from 2016/17 to 2017/18 heating seasons: Attributions and process analysis. *Environmental Pollution, 274*, Article 116523. https://doi.org/10.1016/j.envpol.2021.116523

Zhou, M., Xie, Y., Wang, C., Shen, L., & Mauzerall, D. L. (2024). Impacts of current and climate induced changes in atmospheric stagnation on Indian surface PM2. 5 pollution. *Nature Communications, 15*(1), Article 7448. https://doi.org/10.1016/j.apr.2024.102337